Carbon Letters (2021) 31:1–12
https://doi.org/10.1007/s42823-020-00154-w

Online ISSN 2233-4998
Print ISSN 1976-4251

REVIEW

Graphene quantum dots synthesis and energy application: a review

S. Akash Prabhu[1] · V. Kavithayeni[1] · R. Suganthy[1] · K. Geetha[1]

Received: 7 February 2020 / Revised: 23 April 2020 / Accepted: 12 May 2020 / Published online: 10 June 2020

Abstract
Graphene Quantum Dots (GQDs), zero-dimensional nanoparticles which are derived from carbon-based sources owned the new pavement for the energy storage applications. With the varying synthesis routes, the in-built properties of GQDs are enhanced in different categories like quantum efficiency, nominal size range, and irradiation wavelength which could be applied for the several of energy and optoelectronics applications. GQDs are especially applicable in the specific energy storage devices such as super capacitors, solar cells, and lithium-ion batteries which were demonstrated in this work. This paper critically reviews about the synthesis techniques used for the GQDs involving energy storage applications with increased capacitance, energy conversion, retention capability, and stability.

Keywords Graphene quantum dots (GQDs) · Quantum efficiency · Lithium-ion batteries · Solar cells · Super capacitors · Synthesis routes

1 Introduction

Graphene is an one atom thick 2-D sheet of carbon isotope, recently attracted the researchers due to their discrete chemical, physical, mechanical, and electrical properties like high thermal stability, high electric conductivity with low power dissipation, high-electron mobility of 15,000 $cm^2\ V^{-1}\ s^{-1}$, large surface area, superior flexibility, tunable band gap, quantum confinement effect, and edge effect [1–5]. Due to above properties, graphene is a suitable material for energy applications like lithium-ion battery, hybrid super capacitors, solar cells, and fuel cells [6–8].

In graphene, valance band and conduction band are slightly overlap, which makes it as a zero band-gap semiconductor [4, 9]. Observation of photoluminescence is difficult in graphene sheets, which limits its application in organic LEDs, photodetectors, and photodiodes [2, 10]. However, infinite exciton Bohr radius phenomenon in 0-D graphene quantum dots (GQDs) and 1-D nanoribbon overcomes these limitations and enables their use in above-mentioned applications [11]. The comparison between them is mentioned in Table 1.

Einollahzadeh et al. (2016) reported the simulation study on penta-graphene band structure and energy band gap with Discrete Fourier Transform (DFT) and G_0W_0 approximation were calculated as 2.21–2.336 eV and 4.1–4.3 eV, respectively [12]. RugeQuhe et al. (2013) reported the experimental study on bilayer graphene (BLG) and concluded that the band gap opens to 0.255 eV on bilayer graphene (BLG) and can be fabricated as a Field-Effect Transistor (FET) [13]. The scholars and researchers around the globe have been working on graphene like controlling the size & shape and doping with functional groups to modify the properties of graphene for various applications [3].

Recently, researchers have been focusing on GQDs due to their unique size-dependent luminescence properties which makes it distinct from other carbon derivatives [14, 15]. GQDs also exhibit other excellent properties like high photostability, biocompatibility, low toxicity, tunable fluorescence, high quantum efficiency, and chemical inertness compared to other semiconducting quantum dots [16–19]. GQDs have high potential to be applied in optoelectronics, organic photovoltaics, electronic devices, catalyst, electrochemical application, ion sensing, and bioimaging [16, 17, 20]. In this perspective, we focused on strategic method to synthesis GQDs related with the energy storage and conversion application.

✉ K. Geetha
rktgeetha@gmail.com

[1] Nanotechnology Division, Department of Electronic and Communication Engineering, Periyar Maniammai Institute of Science and Technology, Thanjavur 613403, Tamil Nadu, India

Table 1 Comparison between 2-D, 1-D and 0-D Graphene structure

Material properties	2-D graphene	1-D graphene nanoribbon	0-D graphene quantum dots
Specific surface area	High	High	High (easily get stacks and aggregate)
Thermal stability	High	Medium	Sensitive to temperature on preparation
Electrical stability	High	Medium	Low
Optical stability	Low	Medium	High
Special futures	Tailorable surface chemistry	Abundant edges, high length-to-width ratio and numerous activate sites	Edge effects and quantum confinement

Wen-Wen Liu et al. (2013) reported the study of GQD-based micro-super capacitor prepared by electrochemical deposition. GQDs used in the study have 1.0–5.4 nm size distribution and were synthesized from graphene oxide. GQDs were deposited on gold electrode and the test was carried out in both aqueous electrolyte and ionic liquid electrolyte. The GQD-based micro-super capacitor exhibited excellent rate capability up to 1000 V s^{-1}, and short relaxation time constant of 103.6 µs in aqueous electrolyte and 53.8 µs in ionic liquid electrolyte, and also has a stable life cycle [21]. Zonglong Zhu et al. (2014) reported their study on role of GQDs in perovskite solar cell for faster electron extraction. The GQDs were synthesized by facile electrochemical method having an average diameter of 5–10 nm and were coated as an ultrathin layer between perovskite and Titanium dioxide (TiO_2). The GQDs have improved the power conversion efficiency of solar cell from 8.81% to 10.15% and fast electron extraction time from 260–307 to 90–106 ps [22]. Li Ruiyi et al. (2015) studied the electrochemical performance of lithium titanate/nitrogen and sulfur co-doped graphene quantum dot hybrid to enhance the anode for lithium-ion battery, and they reported that the specific discharge of hybrid lithium-ion battery is 254.2 mAh g^{-1}at 0.1°C and 126.5 mAh g^{-1} at 10°C. The capacity remains at 96.9% for at least 2000 cycles at 2°C [23]. This shows that the GQDs can be used in energy conversion devices, electronics, and optoelectronics for faster electron extraction [22].

2 Synthesis routes

Synthesis of graphene quantum dots (GQDs) is broadly classified into two categories; they are Top-Down and Bottom-Up approach. Top-Down approach is nothing but breaking down from bulk scale to nanoscale. In case of GQDs, the Top-Down approach involves decomposition and exfoliation of carbon derivative precursors like graphene sheet, graphite powder, carbon nanotubes, carbon black, and carbon fiber shown in Fig. 1 [4, 24]. The different types of methods available are hydrothermal or solvothermal cutting, ultrasonicated exfoliation, acidic or plasma oxidation, nanolithography technique, and electrochemical and photo-Fenton reaction.

The Bottom-Up approach is building up from atomic scale to nanoscale. In case of GQDs, this approach uses aromatic compounds like benzene and C60 (fullerene) as precursors, since the shape and size distribution of GQDs can be controlled during their growth. The techniques involves microwave-assisted method, cage opening, and stepwise organic synthesis, as shown in Fig. 2 [4, 24–27].

2.1 Top-down approach

2.1.1 Hydrothermal and solvothermal method

These processes are more effective to synthesize two dimensional quantum dots and also simple and cost effective when compared to other processes [28]. In hydrothermal method, water is used as a solvent, whereas in solvothermal method, organic solution like DimethylFormamide (DMF) is used as a solvent [4, 24, 25]. Pan et al. (2010) synthesized blue luminescent GQDs having an average diameter of 9.6 nm by oxidization of graphene sheets (GSs) and deoxidization of oxidized GSs at low-temperature range of about 200–300 °C [29]. Initially, the precursors were treated with strong oxidizing agents like concentrated sulphuric acid (H_2SO_4) and concentrated nitric acid (HNO_3) at high temperature. The oxidization steps involves creating epoxy (C–O–C), carbonyl (C=O), and carboxylic function group (− COOH) at edge, which rupture and break C–C bond. Furthermore, alkaline hydrothermal reaction tends to remove the epoxy and carbonyl compounds. The carboxylic function groups remain stable at the edge, which is responsible for dispersing GQDs in water. The oxygen atom is removed by further thermal treatment at high temperature of the solution. The selection of temperature in thermal reduction steps has large impact in breaking down the precursor [4, 29]. A group of researchers have reported about the synthesis of green luminescent GQDs of 3.6 nm average diameter from the graphene oxide sheets at high temperature using thermal reduction method [30].

Wang et al. (2014) reported preparation of functionalized GQDs with amine group at average lateral distribution

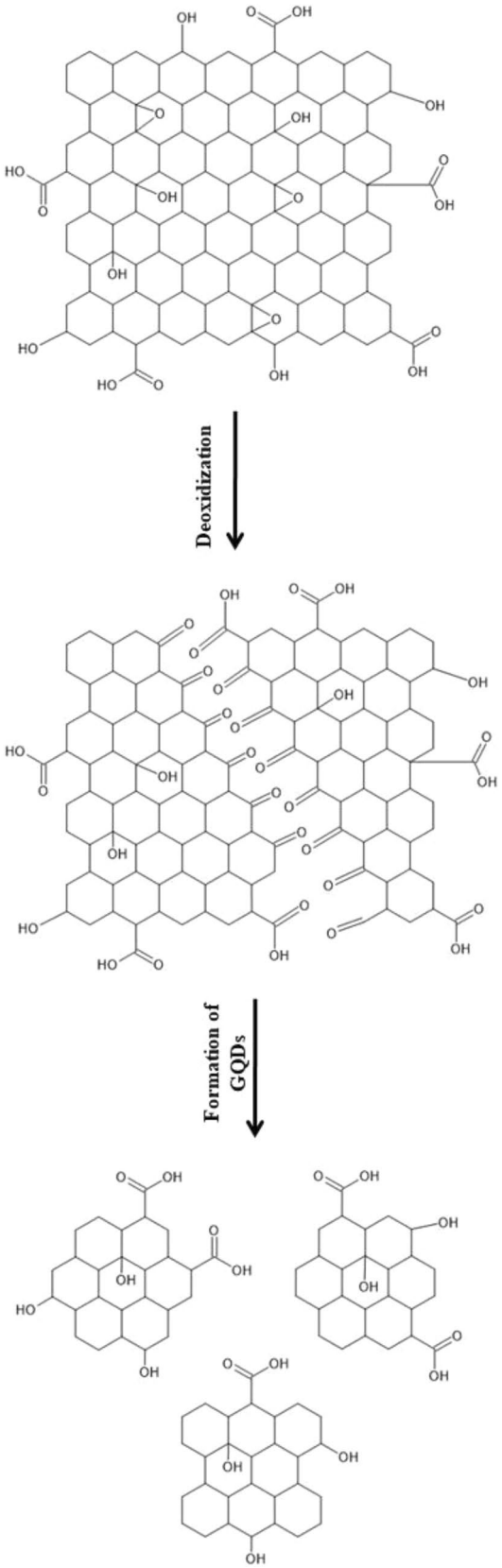

Fig. 1 Top–down approach of GQDs' process

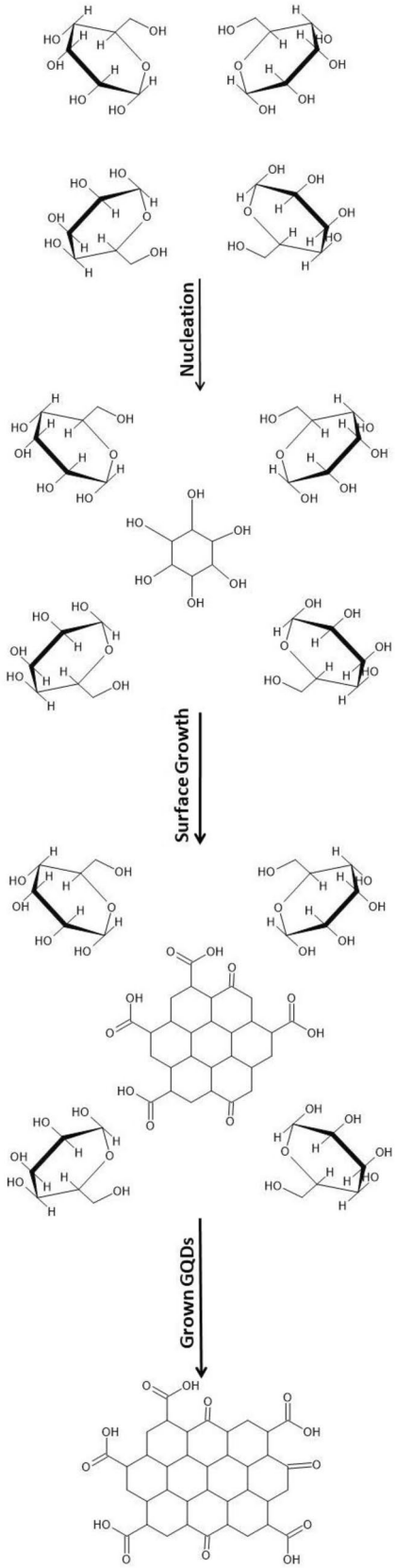

Fig. 2 Bottom–up approach of GQDs' process

of 3.5 ± 0.6 nm with thickness of 1.47 ± 0.86 nm by facile molecular fusion route under mild and green hydrothermal conditions. The synthesis of amine functionalized GQDs involves in nitration of pyrene using nitric acid in alkaline aqueous solution. In this process, alkaline plays an important role in functionalization of GQDs with (−OH, $-NH_2$, and $-NHNH_2$), which is done by intermolecular dehydrolysis in graphene framework [31].

Zhu et al. (2011) synthesized GQDs using DMF as a solvent by one-step solvothermal method. The GQDs have 5.3 nm average diameter with thickness of 1.2 nm. Due to the presence of chemical groups like – OH, epoxy/ether, C=O, and –CO–NR_2, it exhibits excellent solubility of 15 mg/ml in acetone, tetrahydrofuran (THF), DMF, ethanol, dimethyl sulfoxide (DMSO), and water. The synthesized GQDs produced strong luminescence of quantum yield about 11.4% [32]. Liu et al. (2013) synthesized nitrogen-doped GQDs having average diameter of 2.5 nm by solvothermal method. They used graphene oxide (GO) as precursor and DMF as solvent, where DMF undergo decomposition at 200 °C to obtain dimethylamine for nitration of GO for 4–5 h at 200 °C [33]. Even though the hydrothermal and solvothermal methods are very efficient, control of distribution of size and morphology of the GQDs is a drawback in these methods.

2.1.2 Ultrasonic waves assisted

Ultrasonic wave-assisted liquid-phase exfoliation generates altering low- and high-pressure regions in the liquid which induces cavitation that creates hydrodynamic shear forces and high-speed impinging liquid jets into the solution. The force created by the gradient pressure utilized to exfoliate the bulk graphite layers and for the synthesis of GQDs from glucose precursor needs carbonization and polymerization with the same force mentioned. This will help to synthesize GQDs with increase in reaction rate and to reduce edge defects on graphite layers [34–37].

Kumar et al. (2014) synthesized of amine functionalized GQDs by passing ultrasonic waves at 250 W power for 30 min. The size distribution of GQDs was approximately between 5–7 nm and 20–30 nm when using quantum graphene flakes as precursor with the same parameters applied before. Due to p orbital hybridization of C–N atoms at the edge sites make additional inter-band energy of 3.28 eV. Photoluminescence quantum yield was found to be 29% for GQDs and 16% for QGFs, with spectrum excitation at 310 nm. The energy transfer efficiency of GQDs and QGFs is 17% and 15%, respectively [38]. Zhu et al. (2014) synthesized high quantum yield GQDs by one-step ultrasonication synthesis for alkaline phosphatase sensing. The average diameter of GQDs is 3.0 nm with thickness range between 0.7 and 3 nm. The excitation achieved at 380 nm along with emission at 470 nm. The synthesized GQDs have about 27% of quantum yield at pH 7 [39]. Ali et al. (2016) reported GQDs synthesized from graphene flakes through grinding-assisted co-solvent ultrasonication operating at 100 W for 1 h. This involved chemo-mechanical techniques which was mortar grinding and ultrasonication where energy transfer is used to breakdown the graphene nanoplatelets. This method produces GQDs at a diameter range between 2 and 4 nm with lattice space of 2.4 nm. The GQDs gave a strong luminescence at 350 nm with band-gap energy of 2.6 eV [40].

2.1.3 Electrochemical method

This electrochemical method involves use of carbon derivatives such as graphite, CNTs, carbon nanofibres as electrodes, and platinum as the counter electrode. This method lacks to prises the size and surface morphology, and further undergoes filtration and chromatography for separation to obtain monodispersed GQDs. Major drawback of electrochemical synthesis methods is that they have low photoluminescence efficiency on GQDs [41–44].

Zhou et al. (2006) studied blue luminescent nanocrystals (NCs) from multiwalled carbon nanotubes (MWCNTs) by produced by electrochemical method. The size distribution of NCs being 2.8 nm in diameter with spacing distance from 3.1 to 3.4 Å and the quantum yield about 0.064, excited at 340 nm [45]. Zhang et al. (2012) studied highly fluorescent water soluble GQDs from graphite rod through electrochemical method for biological labeling of stem cells. Uniform graphene sheets were observed with size distribution range between 5 and 10 nm providing the interspacing distance about 0.3 nm. By following this method, the strong yellow luminescence could obtain with 14% yield, at the excitation of 540 nm. From this experiment, the GQDs were used to penetrate stem cells for studying the metabolism activity and self-renewability of stem cells without affecting their viability, proliferation, strong photoluminescence, and photostability with low cytotoxicity [46]. Tan et al. (2014) reported small-sized red fluorescent graphene quantum dots as a bioimaging platform synthesized through electrochemical method with uniform size distribution about 3 nm of diameter with 0.24 nm as interspacing distance. The fluorescence decay of GQDs is observed with initial emission of red fluorescence at 600 nm and then emission of yellow fluorescence at 550 nm after 3 h. Six hours later, the emission is converted to green fluorescence at 500 nm. At last after about 12 h, the GQD solution emitted blue fluorescence at 420 nm [47]. Luo et al. synthesized GQDs through electrochemical oxidation of graphene with uniform distribution range of 3–5 nm and thickness of 0.93 nm for single layer graphene sheet. This study reported the synthesis of large size GQDs of about 52 nm diameter, which is purified with dialyzing solution using dialysis bag. The GQDs solution possessed blue emission under 365 nm irradiation [48].

2.2 Comparison between top–down approaches

Form the studies between different top–down processes are analyzed and verified. The deoxidization mechanism is the basic process under-grows in every cutting top–down method of the bulk carbon precursor. The main difference in source involved in the process. Comparing them the hydrothermal process attracted many people due to simple process in the deoxidization. The hydrothermal can further enhanced by addition ultrasonication and electrostatic force. Few more example are given in Table 2.

2.3 Bottom–up approach

2.3.1 Microwave assisted

The microwave-assisted method synthesizes GQDs at a faster rate and homogenous heating is employed with precursors with uniform size distribution. The main advantage is that the GQDs are synthesized without any passivizing agent. The time period of passing microwaves is an important parameter, since increase in time period increases heating time which in turn increases the size of the GQDs, respectively [49–51].

Zhang et al. (2015) produced GQDs using aspartic acid and ammonium bicarbonate NH_4HCO_3 by one-pot microwave-assisted synthesis at 560 W operating power for detection of iron ions and pH. These GQDs have 2.1 average diameter and 14% of quantum yield exhibiting blue luminescence [52]. Zheo et al. reported green fluorescent GQDs derived from deoiled asphalt using one-step microwave-assisted method at 600 W power. The GQDs' size distribution was in the range 1–6 nm, producing green luminescence at 365 nm excitation and high quantum yield up to 14% [53]. Kumawat et al. (2018) reported one-pot microwave-assisted green synthesis route at 900 W for the synthesis of red-luminescent GQDs from ethanol extracts obtained from *Mangifera indiia* (mango) leaves. The size distribution of GQDs synthesized from the extract ranges from 2 to 8 nm and the fluorescence emission was found to be between 650 and 750 nm [54].

2.3.2 Cage opening process

The cage opening process basically uses fullerene C_{60} to produce GQDs by breaking done the covalent bond between carbon atoms by the host molecules.

Chua et al. (2014) reported the study of strong fluorescent GQDs by cage opening Buckminster fullerene. This process undergoes oxidation, cage opening, and fragmentation on C_{60} (fullerene) by strong acid, which produce the GQDs in the sized range of approximate 2–3 nm with 0.6–1 nm height. Show the intensity at 460 under 340 nm excitation wavelength [55].

2.3.3 Stepwise organic synthesis

The solution chemistry synthesis processes provide identical molecular structures to the grapheme which leads to large quantity of production. These molecular modification leads to interact with other complex materials [56–58]. Even though it can produce monodispersed GQDs with uniform size distribution, it cannot prevent GQDs from aggregation caused by the π–π-bond interaction [59].

Yan et al. (2012) reported the study of GQDs synthesized by stepwise organic synthesis method and its mechanism. The polyphenylene dendritic precursor oxidized and make of 168, 132, and 137 conjugated carbons. To make GQDs as more stable due to the 2´, 4´, 6´-triakyl phenyl groups are attached covalently to the ten positions of the graphene moieties [60].

2.4 Comparison between bottom–up approaches

Comparison between bottom–up microwave processes is the attracted method, which involves hydrothermal process irradiated with microwave to form GQDs from carbon derivatives like glucose and starch, however, which lack in size control. To control the size cage opening and step organic synthesis are complimentary to microwave-assisted process. Its lack in low quantum yield and complicated process comparing to microwave-assisted. Due to that, the many researcher scholars are following microwave-assisted and more related reference are given in Table 3.

3 Energy-related applications of GQDs

3.1 Capacitors

Generally, capacitors are classified into two types based on the adsorption/desorption and surface redox reactions. The need for best capacitor material is satisfied with the GQDs, because of the existence properties like high surface area, conductivity, long life stability, rapid adsorption and desorption rate, etc., [74]. Super capacitors which possess specific energy storage and high surface area along persistent cyclic behavior with the help of the charge carriers present which could be applied for on-chip operations in micro-power systems [75]. Integrated power sources for displays, FETs, etc., with transparent look attracted the researchers to move on to GQDS [76, 77]. The highlighted properties of GQDs include optical transparency with nanoscale size, high-electron

Table 2 Top–down synthesis method for GQDs

Method	Material	Precursors	Parameter	Size range (nm)	Quantum yield	Irradiation wavelength (nm)	Ref
Hydrothermal	S, N-GQDs and N-GQDs	Citric acid as C source and urea, thiourea as N, S source	Autoclave at 160 °C for 4 h and centrifuge, 5000 rpm, 5 min	2.69 and 3.10	71% and 78%	340–400 and 420–520	[61]
	GQDs	GO prepared for Graphite (12000 mesh), HNO_3, H_2SO_4	Ultrasonication for 5 h with DI water, centrifuged at 12,000 rpm for 10 min, pH to 12 by KOH and autoclave at 180 °C for 10 h	10–30	–	365	[62]
	C-QD	α-D-Lactose, D-glucose, sucrose, tris(hydroxymethyl) amino-methane (Tris),	Refluxed at 100 °C with stirring for 24 h	1.5	12.5 %	–	[63]
	N-GQDs (green and khaki)	Graphene oxide (GO) in the presence of hydrogen peroxide (H_2O_2) and ammonia	Autoclave and heated at 180 °C for 3 h. and then dialyzed in a dialysis bag (3500 Da) for 48 h	2.1 and 6.2	3.93 % and 2.53 %	310	[64]
	S-GQDs	Molasses, PTFE-lined stainless steel	autoclave and heated at 180 °C for 4 h and sonicated for 2 h	2.9	–	365	[65]
Solvothermal	GQDs	GO powder and *N*, *N*-Dimethylformamide (DMF)	Ultrasonication 500 W for 1 h, autoclave (125 mL) at 200 ℃ for 8 h	1–5	–	280–480	[66]
		GO (< 150 µm), DMF	Ultrasonication for 30 min (120 W, 100 kHz), autoclave (30 mL) and heated at 200 ℃ for 8 h	3.2	–	320	[67]
		GO nanosheets, *N*, *N* dimethylformamide (DMF)	Microwave oven at a power (300, 500, 800 and 1000 W) for (1, 3, 5, 7 and 9 min), After ultrasonic treatment for 2 h and autoclave and heated in for 8 h	5–8	–	486	[68]
Electrochemical	GQDs	Graphite rod	Electrolysis done at NaOH aqueous solution, 80–200 mA cm^2, Pt as counter electrode	5–10	14%	540	[46]
		Graphite and K2S2O8	+ 5.0 V Positional applied to graphite rod in K2S2O8	3	–	420 & 500	[70]

Table 3 Bottom-up approach for GQDs

Method	Material	Precursors	Parameter	Size range (nm)	Quantum yield	Irradiation wavelength (nm)	Ref
Microwave-assisted	N-GQDs	Glucose, urea, and coumarin 1	Microwave oven at 1208 ℃ for 1 min and dialyzed using 3.5-kDa for 75 h	3	5.2 %	–	[69]
	GQDs	Glucose, polyethylene glycol	Microwave power at 595 W for (1, 3, 5, 7, and 9 min)	2	15%	–	[70]
		Aspartic acid and NH_4HCO_3	One-pot microwave-assisted synthesis at 560 W power	2.1	14%	–	[52]
		Deoiled asphalt	Assisted at 600 W microwave power	1–6	14%	365	[53]
Cage-opening method	GQDs	Ethanol extracts obtained from *Mangifera indiia* (mango) leaves	Microwave assisted at 900 W power	2–8	–	650–750	[54]
		Fullerene C_{60}	Synthesis GQDs in presence of sodium nitrate, 98% of H_2SO_4 with potassium permanganate	2–3	–	460	[55]
Stepwise organic synthesis	GQDs	Polyphenylene dendritic	–	–	–	–	[60]
		Natural amino acid, L-glutamic acid	Pyrolyzing L-glutamic acid at 210 ℃	5	54.5%	800 - 850	[71]
		4H nitrogen-doped SiC plates	Pyrolyzing done at 1400–1500 ℃ in presence of hydrogen at 80–160 mTorr	2.58 ± 0.31	–	–	[72]
	N-GQDs	1,3,5-triamino-2,4,6-trinitrobenzene (TATB)	TATB was raised to 750 ℃ at a ramping rate of 2 ℃ min^{-1} under a nitrogen atmosphere	2–5	–	460–540	[73]

mobility, and elevated strength along with additional micro pores expanded its capacitance power [78–81].

Complete discussion of Table 4. Keunsik et al. (2016) reported the high capacitance performance of GQD-based supercapacitors fabricated by simple electrophoretic method about 9.09 μF cm^{-2} with optical transparency of 92.97% and 550 nm [75]. Sanjoy et al. (2015) reported, in his study, about the high capacitance retention of 80% over 3000 cycles which had been obtained through the introduction of 6.0 nm-sized GQDs with a capacitance range of 1044 Fg^{-1}

Table 4 GQDs for capacitor

S.No	Material	Method	Application	Size (nm)	Retention/capacity	Stability (cycles)	References
1	GQDs	Electrophoretic method	Capacitor	550	9.09 μF cm^{-2}	–	[75]
2	GQDs	One-step solvothermal method		–	1107.4 μF cm^{-2}	a-	[82]
3	GQDs	–		6.0	80%	3000	[83]
4	GQDs	Top–down strategy		–	307.6 F g^{-1}	5000	[84]
5	GQDs	Ultrasonication assisted		2–4.5	99%/1242 F g^{-1}	4000	[85]
6	S,N-GQDs	Hydrothermal		3–7	100%/2524 F g^{-1}	1000	[86]
7	GQDs	–		–	82.36%/1526 F g^{-1}	–	[87]
8	GQDs	–		–	96%/361.97 F g^{-1}	1000	[88]

[82]. Wen-wen liu et al. (2013) mentioned in his work about GQD-based micro-capacitors synthesized by one-step solvo thermal method which exhibits capacitance and density of energy in 1107.4 μF cm^{-2} and 0. 154 μWh cm^{-2}. [83]. GQDs fabricated via a new method of top–down strategy which has shown the density of energy value as 41.2 W h kg^{-1} with high capacitance of 307.6 F g^{-1} and outstanding retention capacitance even after 5000 cycles had been reported by Zhang Shuo et al. (2018) [84]. Jiahuan Luo et al. (2019) demonstrated the excellent specific capacitance of tremella-shaped $NiCo_2O_4$ encapsulated by graphene quantum dots (GQDs) and specific energy density of asymmetric supercapacitor. They have been synthesized GQDs by solvothermal assisted by ultrasonicated and confirm the uniform size distribution of 2—4.5 nm with 0.21 nm interlayer spacing by HR-TEM. The GQDs encapsulate $NiCo_2O_4$ by annealing at 300 ℃ for 24 h. They have compared the specific capacitance of pristine $NiCo_2O_4$ and $NiCo_2O_4$@GQDs. $NiCo_2O_4$@GQDs exhibit 1242 F g^{-1} at 30 A g^{-1} in 2.0 M KOH, which show 57% enhanced specific capacitance compared to pristine $NiCo_2O_4$ (790 F g^{-1} at 30 A g^{-1}) and 99% retention capacitance after 4000 cycles. Asymmetric supercapacitor (ASC) is fabricated by pairing NiCo2O4@GQDs and activated carbon (AC) as positive electrode and negative electrode. Its shows enhanced specific energy density is as high as 38 W h kg^{-1} at a power density of 800 W kg^{-1} [85].

3.2 Solar cells

From the conventional Si wafers to metal oxide, lead-based composite wafers had been used in solar cells with low power conversion efficiency which moves forward the solar cells for GQD-based wafers [89]. Silicon, perovskite, and TiO_2-based solar cells are moving in a broad way of research due to its biocompatible nature, chemical stability, and low cost [90–92]. The GQDs indulged in solar cells applications exhibited the properties like hole/electron transport, additive active layer in the donar and acceptor blends, and as a sensitizer too [93, 94]. While comparing with TiO_2 and CdSe-based quantum dots, GQDs enhances the solar cell efficiency by the existence of quantum confinement along size specified band gap, hot-electron lifetime, and ultrafast electron extraction with distinctive optical and electrical transport properties [95–97].

Briefing of Table 5, Travis G. Noval et al. (2016) mentioned in his study about the PEG functionalized GQDs application on solar cells with an improved efficacy of 36% along the conversion energy of 6.63% [98]. Zonglong Zhu et al. (2014) reported in his study about the ultrathin GQDs layer which is sandwiched between the perovskite solar cell and mesoporous titanium dioxide increases its efficiency of greater than 10%, where before it was only 8.81% without the presence of GQDs [99]. Senlin Diao et al. (2017) reported the GQDs as an excellent heterojunction solar cell with optimal efficiency of 12.35% about 20 nm thickness along with the remarkable physical and chemical stability [89]. Liu et al. (2017) mentioned in his study about the electrochemical stability and efficiency of $SrRuO_3$ encoded GQDs of about 8.05% than before encoded [100].

3.2.1 Lithium-ion batteries

Lithium-ion-based batteries are having the specific capacity and a remarkable energy source which could be applied in electric vehicles, defense, smart electric grids, and other electronic devices [105, 106]. The foremost properties of Li-ion batteries like long cycle usage without memory effect and high power density made it as a noticeable chemical energy storage device [107]. Li-ion batteries almost reached the capacity level up to 2.6 $mAhg^{-1}$ than the conventional one and also possesses high-quality lithium-ion cells for consumer use also [108].

Briefing of Table 6, Chao et al. (2015) reported in his study about the GQDs anchored VO_2 electrode arrays exhibits the retention percentage of 94 for 1500 cycles with 36% capacitance and 389 $mAhg^{-1}$ capacity, while GQDs was used as a anode material [109]. Li Ruiyi et al. (2015) mentioned in his study about the electrochemical performance of sulfur co-doped GQDs, with a specific discharge capacity of 254 2$mAhg^{-1}$, involves 2000 cycles at 2C along with retention percentage of 96.9 [110].

Table 5 GQDs for solar cell

S. No	Material	Method	Solar cell type	Conv Eff (%)	References
1	GQDs	Hydrothermal	Solar cell	12.35	[89]
2	GQDs	GICs	Organic	6.63	[98]
2	GQDs/TiO_2	Electrolysis	Perovskite	8.81	[99]
3	GQDs/$SrRuO_3$	Hydrothermal	Dye-sensitized	8.05	[100]
4	PANI–GQDs	Sono–Fenton method	Plastic solar cell	0.86	[101]
5	SnO_2:GQDs	–	Perovskite	21.1	[102]
6	N-GQDs	–	Perovskite	16	[103]
7	GQDs	–	Dye-sensitized	4.58	[104]

Table 6 GQDs for lithium-ion battery

S.No	Material	Method	Application	Retention	Capacity/stability	Ref
1	GQDs/ VO_2	Self-assembly	Lithium-ion batteries	94%	389 $mAhg^{-1}$/1500 cycles	[109]
2	GQDs	Microwave-assisted		96.9%	254.2 $mAhg^{-1}$/2000 cycles	[110]
3	N-GQDs	Hydrothermal		–	161 $mAhg^{-1}$/500 cycles	[111]
4	GH-BGQD	Hydrothermal		–	687 $mAhg^{-1}$/70 h	[112]
5	NiO@Co_3O_4@GQDs	–		76%	1158 $mAhg^{-1}$/3000 cycles	[113]

4 Conclusion

In this review, our perspective have discussed various synthesis techniques and its relevant application of GQDs. Top-down and bottom-up approaches utilized for the synthesis, provides optimized and unique quantum yield for the GQDs, have been demonstrated through this work. Comparing with the bottom-up approaches, hydrothermal-assisted techniques under top-down approach possessed the highest quantum yield of 78% and particle-size range of 2–3 nm. The factor affecting GQDs such as shape, size, surface effect, doped material, etc., have still in an unclear condition in accordance with theoretical evaluation. When it comes to large production of GQDs, uniformity has been a great challenging, because synthesis of GQDs involves multiple steps. The developments in synthesis process have great concern.

10% of references have taken from past 2 years, which enlighten the GQDs current energy-based application. The multi-tasking ability of GQDs such as quantum efficacy with inert chemical nature, etc., which could made it applicable in different fields of electronics and energy applications. Electrophoretic method fabricated supercapacitors using GQDs provides the highest capacitance and optical transparency of 92.97%. SnO2 helps perovskite solar cell for enhance energy conversion efficiency up to 21.1% due to the incorporated GQDs were reported [102]. The current research moves onto a another leap, which plastic solar made up of polyaniline–GQDs nanocomposite with energy conversion up to 0.86%, reported by Firoz Khan et al. (2020) [101]. GQDs applied lithium-ion batteries exhibited the highest retention efficacy of 94% and 97% and possessed stability over 1500 cycles and above. In the other hand, Xiaojie Yin fabricated new type battery with NiO@Co3O4@GQDs composite material which exhibit excellent specific capacitance 1158 mAhg-1 with 76% retention over 3000 cycles. Thus, GQDs are the best and novelized way for building energy-based applications.

By the obtained literature reviews, GQDs an exceptional material gained with ease of synthesis provoked a tremendous change in energy-based application. Being a 0-D nanomaterial, it has been put forth into organic semiconducting QDs. Moreover, GQDs started an ear in the advance material and applied technologies for the further development in science.

Author contributions APS, KV, and SR are equally contributing their effort to draft the manuscript. GK^{2*} reviewed and corrected the manuscript. All authors read and approved the final manuscript.

Funding Not applicable.

Data availability Not applicable.

Compliance with ethical standards

Conflict of interests The authors declare that they have no competing interests.

References

1. Bak S, Kim D, Lee H (2016) Graphene Quantum dots and their possible energy application: a review. Curr Appl Phys 16(9):1192–1201
2. Feng J, Dong H, Yu L, Dong L (2017) Optical and electronic properties of graphene quantum dots with qxygen-containing groups: a dendity functional theory study. J Mater Chem C 5(24):5984–5993
3. Wei D, Liu Y (2010) Controllable synthesis of graphene and its application. Adv Mater 22(30):3225–3241
4. Bacon M, Bradley SJ, Nann T (2013) Graphene quantum dots. Adv Mater 31(4):415–428
5. Changcheng Jiang ZD, Cheng H, Zhao Y, Shi G, Jiang L, Qu L (2012) Facile fabrication of light, flexible and multifunctional graphene fibers. Adv Mater.
6. Yu L, Wu HB, Lou XWD (2017) Self-Templated Formation of Hollow Structures. Acc Chem Res. 50(2):293–301
7. XiaomingLi MR, Song J, Shen Z, Zeng H (2015) Carbon and graphene quantum dots for optoelectronic and energy devices: a review. Adv Funct Mater 25:4929–4947
8. Bonaccorso F, Colombo L, Yu G, Stoller M, Tozzini V, Ferrari AC, Ruoff RS, Pellegrini V (2015) Graphene, related two-dimensional crystals, and hybrid systems for energy conversion and storage. Science 347(6217):1246501
9. Geim AK, Novoselov KS (2007) The rise of graphene. Nature Mater 6:183–191
10. Mueller T, Xia F, Avouris P (2010) Graphene photodetectors for high-speed optical communications. Nat Photonics 4:297–301
11. Gupta S, Smith T, Banaszak A, Boeckl J (2017) Graphene quantum dots electrochemistry and sensitive electrocatalytic glucose sensor development. Nanomaterials 7:301

12. Elinollahzadeh H, Dariani RS, Fazeli SM (2016) Computing the band structure and energy gap of penta-graphene by using DFT and G_0W_0 approximation. Solid State Communication 229:1–4
13. Quhe R, Ma J, Zeng Z, Tang K, Zheng J, Wang Y, Ni Z, Wang L, Gao Z, Shi J, Ju J (2013) Tunable band gap in few-layer graphene by surface adsorption. Scientific Reports 3, Article number: 1796.
14. Kim S, Hwang SW, Kim M-K, Shin DY, Shin DH, Kim CO, Yang SB, Park JH, Hwang E, Choi S-H, Ko G, Sim S, Sne C, Choi HJ, Bae S, Hong BH (2012) Anomalous behaviors of visible luminesecence from graphene quantum dots: interplay between size and shape. ACS Nano 6(9):8203–8208
15. Geim AK (2009) Graphene: status and prospects. Science 324(5934):1530–1534
16. Tian P, Tang L, Teng KS, Lau SP (2018) Graphene quantum dots from chemistry to applications. Materials Today Chemistry 10(2018):221–258
17. Gong L, Yang R, Liu R, Chen L, Yan Y, Feng Z (2019) Application of graphene quantum dots in energy storage devices. Progress Chem 31(7):1020–1030
18. Yan Y, Gong J, Chen J, Zeng Z, Huang W, Kanyi Pu, Liu J, Chen P (2019) Recent advances on graphene quantum dots: from chemistry and physics to applications. Adv Mater 2019(31):1808283
19. Ran C, Wang M, Gao W, Yang Z, Shao J, Deng J, Song X (2014) A general route to enhance the fluorescence of graphene quantum dots by Ag nanoparticles. RSC Adv 4:21772
20. Karimzadeh A, Hasanzadeh M, Shadjou N, de la Guardia M (2018) Optical bio (sensing) using nitrogen doped graphene quantum dots: recent advances and future challenges. TrAC Trends Anal Chem 108:110–121
21. Liu W-W, Feng Y-Q, Yan X-B, Chen J-T, Xue Q-J (2013) Superior micro-supercapacitors based on graphene quantum dots. Adv Funct Mater 23:4111–4122
22. Zhu Z, Ma J, Wang Z, Cheng Mu, Fan Z, Lili Du, Bai Y, Fan L, Yan He, Phillips DL, Yang S (2014) Efficience enhancement of perovskite solar cells through fast electron: the role of graphene quantum dots. J Am Chem Soc 136:3760–3763
23. Ruiyi Li, Yuanyuan J, Xiaoyan Z, Li Zaijun Gu, Zhiguo WG, Junkang L (2015) Significantly enhanced electrochemical performance of lithium titanate anode for lithium ion battery by the hybrid of nitrogen and sulfur co-doped graphene quantum dots". Electrochim Acta 178:303–311
24. Kwon W, Rhee S-W (2012) Facile synthesis of graphitic carbon quantum dots with size tenability and uniformity using reverse micelles. Chem Commun 48:5256
25. Lin L, Xu Y, Zhang S, Ross IM, Ong A, Allwood DA (2014) Fabrication and luminescence of monolayered boron nitride quantum dots. Small 10:60
26. Sun Y-P, Zhou B, Lin Y, Wang W, Fernando KS, Pathak P, Meziani MJ, Harruff BA, Wang X, Wang H, J. (2006) Quantum-sized carbon dots for bright and colorful photoluminescence. Am Chem Soc 128:7756
27. Liu R, Wu D, Feng X, Müllen K (2011) Bottom-up fabrication of photoluminescent graphene quantum dots with uniform morphology. J Am Chem Soc 133:15221
28. Buzaglo M, Shtein M, Regev O (2015) Graphene quantum dots produced by microfluidization. Chem Mater 28:21
29. Pan D, Zhang J, Li Z, Minghong Wu (2010) Hydrothermal route for cutting graphene sheets into blue-luminescent graphene quantum dots. Adv Mater 2010(22):734–738
30. Sofer Z, Bouša D, Luxa J, Mazanek V, Pumera M (2016) Few-layer black phosphorus nanoparticle. Chem Commun 52:1563
31. Wang L, Wang Y, Xu T, Liao H, Yao C, Liu Y, Li Z, Chen Z, Pan D, Sun L, Wu M (2014) Gram-scale synthesis of single-crystalline graphene quantum dots with superior optical properties. Nat Commun 5:5357
32. Zhu S, Zhang J, Qiao C, Tang S, Li Y, Yuan AW, Li B, Tian L, Liu F, Hu R, Gao H, Wei H, Zhang H, Sun AH, Yang B (2011) Strongly green-photoluminescent graphene quantum dots for bioimaging applications. Chem Commun 47:6858–6860
33. Q Liu, B Guo, Z Rao, B Zhang, JR Gong (2013) Strong two-photon-induced fluorescence from photostable, biocompatible nitrogen-doped graphene quantum dots for cellular and deep-tissue imaging. Nano Lett.
34. Hernandez Y, Nicolosi V, Lotya M, Blighe FM, Sun Z, De S, Mcgovern T, Holland B, M Byrne, Gun'ko YK, Boland JJ, Niraj P, Duesberg G, Krishnamurthy S, Goodhue R, Hutchison J, Scardaci V, Ferrari AC, Coleman JN (2008) High-yield production of graphene by liquid-phase exfoliation of graphite. Nat Nanotechnol 3:563–568
35. Li H, He X, Liu Y, Huang H, Lian S, Lee S-T, Kang Z (2011) One-step ultrasonic synthesis of water-soluble carbon nanoparticles with excellent photoluminescent properties. Carbon 49:605–609
36. Paton KR et al. (2014) Scalable production of large quantities of defect-free few-layer graphene by shear-exfoliation in liquids. Nat Mater 13:624–630
37. Lu L, Zhu Y, Shi C, Pei YT (2016) Large-scale synthesis of defects-selective graphene quantum dots by ultrasonic assisted liquid-phase exfoliation. Carbon 109:373–383
38. G. Sandeep Kumar, Rajarshi Roy, Dipayan Sen, Uttam Kumar Ghorai, Ranjit Thapa, Nilesh Mazumder, SubhajitSaha and Kalyan K. Chattopadhyay, (2014), Amino-functionalized graphene quantum dots: origin of tunable heterogeneous photoluminescence, Nanoscale, 6, 3384
39. Zhu Y, Wang G, Jiang H, Chen L, Zhang X (2014) One-step ultrasonic synthesis of graphene quantum dots with high quantum yield and its application in sensing of alkaline phosphatas. Chem Comm 51:948–951
40. Ali J, Siddiqui G-U-D, Yang YJ, Lee KT, Um K, Choi KH (2016) Direct synthesis of graphene quantum dots from multilayer graphene flakes through grinding assisted co-solvent ultrasonication for all-printed resistive switching array. RSC Advances 6:5068–5078
41. Deng J, Qiujun Lu, Mi N, Li H, Liu M, Mancai Xu, Tan L, QingjiXie YZ, Yao S (2014) Electrochemical synthesis of carbon nanodots directly from alcohols. Chem Eur J 20:4993–4999
42. Li H, Kang Z, Liu Y, Lee S-T (2012) Carbon nanodots: synthesis, properties and applications. J Mater Chem 22:24230
43. Li Y, Yue Hu, Zhao Y, Shi G, Deng L, Hou Y, Liangti Qu (2011) An electrochemical avenue to green-luminescent graphene quantum dots as potential electron-acceptors for photovoltaics. Adv Mater 23:776–780
44. Zhu S, Song Y, Zhao X, Shao J, Zhang J, Yang B (2015) The photoluminescence mechanism in carbon dots (graphene quantum dots, carbon nanodots, and polymer dots): Current state and future perspective. Nano Research 8(2):355–381
45. Zhou J, Booker C, Li R, Zhou X, Sham T-K, Sun X, Ding Z (2007) An electrochemical avenue to blue luminescent nanocrystals from multiwalled carbon nanotubes (MWCNTs). J Am Chem Soc 129:744–745
46. Zhang M, Bai L, Shang W, Wenjing Xie A, Ma H, Fu Y, DecaiFang A, Sun AH, Fan L, Han M, Liub C, Yang S (2012), Facile synthesis of water-soluble, highly fluorescent graphene quantum dots as a robust biological label for stem cells, J Mater Chem 22:7461
47. Tan X, Li Y, Li X, Zhou S, Fan L, Yang S (2015) Electrochemical synthesis of small-sized red fluorescent graphene quantum dots as a bioimaging platform. Chem Commun 51:2544–2546
48. Luo P, Guan X, Yu Y, Li X (2017) New insight into electrooxidation of graphene into graphene quantum dots. Chem Phys Lett 690:129–132

49. Tang L, Ji R, Cao X, Lin J, Jiang H, Li X, Teng KS, Luk CM, Zeng S, Hao J, Lau SP (2012) Deep ultraviolet photoluminescence of water-soluble self-passivated graphene quantum dots. ACS Nano 6(6):5102–5110
50. Huang Z, Lin F, Ming Hu, Li C, Ting Xu, Chen C, Guo X (2014) Carbon dots with tunable emission, controllable size and their application for sensing hypochlorous acid. J Lumin 151:100–105
51. Umrao S, Jang M-H, Oh J-H, Kim G, Sahoo S, Cho Y-H, Srivastva A, Oh Il-K (2015) Microwave bottom-up route for size-tunable and switchable photoluminescent graphene quantum dots using acetylacetone: new platform for enzyme-free detection of hydrogen peroxide. Carbon 81:514–524
52. Zhang C, Cui Y, Song L, Liu X, Hu Z (2015) Microwave assisted one-pot synthesis of graphene quantum dots as highly sensitive fluorescent probes for detection of iron ions and pH value. Talanta 150:54–60
53. Zhao P, Li C, Yang M (2016) Microwave assisted one-pot conversion fromdeoiled asphalt to green fluorescent graphene quantum dots and their interfacial properties. J Dispersion Sci Technol ISSN 0193–2691:1532–2351
54. Kumawat MK, Thakur M, Gurung RB, Srivastava R (2017) Graphene quantum dots from mangiferaindica: application in near infrared bioimaging and intracellular nanothermometry. ACS Sustain Chem Eng 5:1382–1391
55. Chun Kiang Chua, ZdenekSofer, Petr Simek, OndrejJankovsky, KaterinaKlı´mova´, SnejanaBakardjieva, St epa´nkaHrdlickova´ Kuckova´, and Martin Pumera, (2014), Synthesis of Strongly Fluorescent Graphene Quantum Dots by Cage-Opening Buckminsterfullerene, ACS Nano
56. Allen MJ, Tung VC, Kaner RB (2010) Honeycomb carbon: a review of graphene. Chem Rev 110:132–145
57. Li L-S, Yan X (2010) Colloidal graphene quantum dots". J Phys Chem Lett 1:2572–2576
58. Xin Ting Zheng ,ArundithiAnanthanarayanan , Kathy Qian Luo , and Peng Chen, (2015), Glowing Graphene Quantum Dots and Carbon Dots: Properties, Syntheses, and Biological Applications, small, 11, No. 14, 1620–1636
59. Yan X, Cui X, Li B, Li L-S (2010) Large, solution-processable graphene quantum dots as light absorbers for photovoltaics. Nano Lett 10:1869–1873
60. Yan X, Li B, Li L-S (2012) colloidal graphene quantum dots with well-defined structures. Account Chem Res 46(10):2254–2262
61. Qu D, Zheng M, Du P, Zhou Y, Zhang L, Li D, Tan H, Zhao Z, Xie Z, Sun Z (2013) Highly luminescent S, N co-doped graphene quantum dots with broad visible absorption bands for visible light photocatalyst. Nanoscale 5:12272–12277
62. Wang F, Zhenyan Gu, Lei Wu, Wang W, Xia X, Hao Q (2014) Graphene quantum dots as a fluorescent sensing platform for highly efficient detection of copper(II) ions. Sens Actuators B 190:516–522
63. Zhang Y-Y, Wu M, Wang Y-Q, He X-W, Li W-Y, Feng X-Z (2013) A new hydrothermal refluxing route to strong fluorescent carbon dots and its application as fluorescent imaging agent. Talanta 117:196–202
64. Zhu X, XiaoxiZuo RH, Xiao X, Liang Y, Nan J (2014) Hydrothermal synthesis of two photoluminescent nitrogen-doped graphene quantum dots emitted green and khaki luminescenc. Mater Chem Phys 147:963–967
65. Sangam S et al (2018) Sustainable synthesis of single crystalline sulphur-doped graphene quantum dots for bioimaging and beyond. Green Chem 20:4245–4259
66. Yang B, Chen J, Cui L, Liu W (2015) Enhanced photocurrent of ZnO nanorods array sensitized with graphene quantum dots, Electron Suppl Material (ESI).
67. Zhu S, Zhang J, Tang S, Qiao C, Wang L, Wang H, Liu X, Li B, Li Y, Yu W, Wang X, Sun H, Yang B (2012) Surface chemistry routes to modulate the photoluminescence of graphene quantum dots: from fluorescence mechanism to up-conversion bioimaging applications, Adv Funct Mater.
68. Dong LM, Shi DY, Wu Z, Li Q, Han ZD (2015) Improved solvothermal method for cutting graphene oxide into graphene quantum dots. Digest J Nanomaterials Biostruct 10(3):855–864
69. Hou X, Li Y, Zhao C (2015) Microwave-assisted synthesis of nitrogen-doped multi-layer graphene quantum dots with oxygen-rich functional groups. Aust J Chem 69(3):357–360
70. LibinTang RJ, Li X, Teng KS, Lau SP (2013) Size-dependent structural and optical characteristicsof glucose-derived graphene quantum dots. Part Part Syst Charact 30:523–531
71. Xu Wu, Tian F, Wang W, Chen J (2013) Min Wu and Julia Xiaojun Zhao, "Fabrication of highly fluorescent graphene quantum dots using L-glutamic acid for in vitro/in vivo imaging and sensing". J Mater Chem C 1:4676
72. Lee NE, Lee SY, Lim HS, Yoo SH, Cho SO (2020) A novel route to high-quality grapheme quantum dots by hydrogen-assistedpyrolysis of silicon carbide. Nanomaterials 10:277
73. Li R, Liu Y, Li Z, Shen J, Yang Y, Cui X, Yang G (2016) Bottom-up fabrication of single-layered nitrogen doped graphene quantum dots through intermolecular carbonization arrayed in a 2D plane. Chem Eur J 22:272–278
74. Bak S, Kim D, Lee H (2016) Graphene quantum dots and their possible energy applications: a review. Curr Appl Phys 16:1192–1201
75. Lee K et al (2016) Highly transparent and flexible supercapacitors using graphene-graphene quantum dots chelate. Nano Energy 26:746–754
76. Jung HY et al (2012) Transparent, flexible supercapacitors from nano-engineered carbon films. Scientific reports 2:773
77. Chen T et al (2014) High-performance transparent and stretchable all-solid supercapacitors based on highly aligned carbon nanotube sheets. Sci Rep 4:3612
78. El-Kady MF et al (2012) Laser scribing of high-performance and flexible graphene-based electrochemical capacitors. Science 335:1326–2133
79. Stoller MD et al (2008) Graphene-based ultracapacitors. Nano Lett 8:3498–3502
80. El-Kady MF, Kaner RB (2013) Scalable fabrication of high-power graphene micro-supercapacitors for flexible and on-chip energy storage. Nat Commun 4:2446
81. Chen Q et al (2014) Graphene quantum dots–three-dimensional graphene composites for high-performance supercapacitors. Phys Chem Chem Phys 16:19307–19313
82. Sanjoy M, Rana U, Malik S (2015) Graphene quantum dot-doped polyaniline nanofiber as high performance supercapacitor electrode materials, Chemical Communications, vol. 51, pp. 12365–12368
83. Liu WW et al, (2013), Superior micro supercapacitors based on graphene quantum dots, Advanced Functional Materials, vol. 23, pp. 4111–4122
84. Shuo Z et al (2018) High-performance supercapacitor of graphene quantum dots with uniform sizes. ACS Appl Materials Interfaces 10:12983–12991
85. Luo J, Wang J, Liu S, Wu W, Jia T, Yang Z, Mu S, Huang Y (2019) Graphene quantum dots encapsulated tremella-like NiCo2O4 for advanced asymmetric supercapacitors. Carbon 146:1–8
86. Abdallah Ramadan M, Anas SE, Soliman M, Abou-Aly A (2020) Effect of co-doped graphene quantum dots to polyaniline ratio on performance of supercapacitor. J Mater Sci 2020(31):7247–7259
87. Qiu H, Sun X, An S, Lan D, Cui J, Zhang Y, He W (2020) Microwave synthesis of histidine-functionalized graphene quantum dots/Ni-Co LDH with flower ball structure for supercapacitor. J Colloid Interface Sci 567:264–273

88. Abidin SNJSZ, Shuhazlly Mamat Md, Rasyid SA, Zainal Z, Sulaiman Y (2015) Electropolymerization of poly(3,4 ethylenedioxythiophene) onto polyvinyl alcohol graphene quantum dot-cobalt oxide nanofiber composite for high-performance supercapacitor. Electrochim Acta 261:548–558
89. Senlin D et al (2017) 12.35% efficient graphene quantum dots/silicon heterojunction solar cells using graphene transparent electrode. Nano Energy 31:P359–366
90. Yan X, Cui X, Li B, Li L (2010) Large solution-processable graphene quantum dotsas light absorbers for photovoltaics. Nano Lett 10:1869–1873
91. Chen L, Guo CX, Zhang Q, Lei Y, Xie J, Ee S et al (2013) Graphene quantum-dotdopedpolypyrrole counter electrode for high-performance dye-sensitized solar cells. ACS Appl Mater Interfaces 5:2047–2052
92. Wang Y, Hu A (2014) Carbon quantum dots: synthesis, properties and applications. J Mater Chem C 2:6921–6939
93. Kim JK, Park MJ, Kim SJ, Wang DH, Cho SP, Bae S et al (2013) Balancing lightabsorptivity and carrier conductivity of graphene quantum dots for highefficiencybulk heterojunction solar cells. ACS Nano 7:7207–7212
94. Li M, Ni W, Kan B, Wan X, Zhang L, Zhang Q et al (2013) Graphene quantum dotsas the hole transport layer material for high-performance organic solar cells. Phys Chem Chem Phys 15:18973–18978
95. Zhang Z et al (2012) Graphene quantum dots: an emerging material for energy-related applications and beyond. Energy Environ Sci 5:8869–8890
96. Lee D, Seo J, Zhu X, Lee J, Shin HJ, Cole JM, Su (2013) Quantum confinement-induced tunable exciton states in graphene oxide. Scientific reports, vol. 3, pp. 2250
97. Williams KJ et al (2013) Hot electron injection from graphene quantum dots to TiO2. ACS Nano 7:1388–1394
98. Novak TG et al (2016) Fast P3HT exciton dissociation and absorption enhancement of organic solar cells by PEG-functionalized graphene quantum dots. Small 12:994–999
99. Zonglong Z et al (2014) Efficiency enhancement of perovskite solar cells through fast electron extraction: the role of graphene quantum dots. J Am Chem Soc 136:3760–3763.
100. Liu T et al (2017) A graphene quantum dot decorated $SrRuO_3$ mesoporous film as an efficient counter electrode for high-performance dye-sensitized solar cells. J Materials Chem A 5:17848–17855
101. Gebreegziabher GG, Asemahegne AS, Ayele DW, Mani D, Sahu RNPP, Kumar A (2020) Polyaniline–graphene quantum dots (PANI–GQDs) hybrid for plastic solar cell. Carbon Lett 30(1):1–11
102. Pang S, Zhang C, Zhang H, Dong H, Chen D, Zhu W, Xi He, Chang J, Lin Z, Zhang J, Hao Y (2020) Boosting performance of perovskite solar cells with graphene quantum dots decorated SnO_2 electron transport layers. Appl Surf Sci 507:145099
103. Bian H, Wang Q, Yang S, Yan DC, Wang H, Liang L, Jin Z, Wang G, Liu SF (2019) Nitrogen-doped graphene quantum dots for 80% photoluminescence quantum yield for inorganic γ-CsPbI3 perovskite solar cells with efficiencybeyond 16%. J Mater Chem A 7:5740
104. Porfarzollah A, Mohammad-Rezaei R, Bagheri M (2020) Ionic liquid-functionalized graphene quantum dots as an efficient quasi-solid-state electrolyte for dye-sensitized solar cells. J Mater Sci 31:2288–2297
105. Vlad A et al (2015) Design considerations for unconventional electrochemical energy storage architectures. Adv Energy Materials 5:1402115
106. Chen YM et al (2018) Minimization of Ion-solvent clusters in gel electrolytes containing graphene oxide quantum dots for lithium/ion batteries. Small 14:1703571
107. Meng J et al (2017) Advances in structure and property optimizations of battery electrode materials. Joule.
108. Choi NS et al (2012) Challenges facing lithium batteries and electrical double-layer capacitors. Angewandte Chemie Int Edition 51:9994–10024
109. Chao D et al (2014) Graphene quantum dots coated VO2 arrays for highly durable electrodes for Li and Na ion batteries. Nano Lett 15(1):565–573
110. Ruiyi Li et al (2015) Significantly enhanced electrochemical performance of lithium titanate anode for lithium ion batterybythe hybrid of nitrogen and sulfur co-doped graphene quantum dots. Electrochim Acta 178:303–311
111. Khan F, Oh M, Kim JH (2019) N-functionalized graphene quantum dots: charge transporting layer for high-rate and durable Li4Ti5O12-based Li-ion battery. Chem Eng J 369:1024–1033
112. Van Tam T, Kang SG, Kim MH, Lee SG, Hur SH, Chung JS, Choi WM (2019) Novel graphene hydrogel/b-doped graphene quantum dots composites as trifunctional electrocatalysts for zn-air batteries and overall water splitting. Adv Energy Mater 9:1900945
113. Yin X, Zhi C, Sun W, Lv L-P, Wang Y (2019) Multilayer NiO@Co3O4@graphene quantum dots hollow spheres for high-performance lithium-ion batteries and supercapacitors. J Mater Chem A 7:7800